Hypercompact HII Regions

Susana Lizano, CRyA-UNAM

Hypercompact (HC) HII regions are very small ionized regions around massive stars

- sizes $R \lesssim 0.01$ pc,
- $EM \gtrsim 10^8$ cm^{-6} pc,
- rising continuum spectra $S_\nu \propto \nu^\alpha$, with $\alpha \sim 1$,
- many of them have broad radio recombination lines with $\Delta v > 40 \mathrm{km\,s^{-1}}$ (e.g., Sewilo et al. 2004).

In is possible that hypercompact HII regions trace very early stages of massive star formation (post the hot molecular core phase). Thus, physical properties (e.g., n, R, morphology, and kinematics) of these regions will help determine the conditions in which massive star are formed and/or the processes that occur at very early stages in their lives.

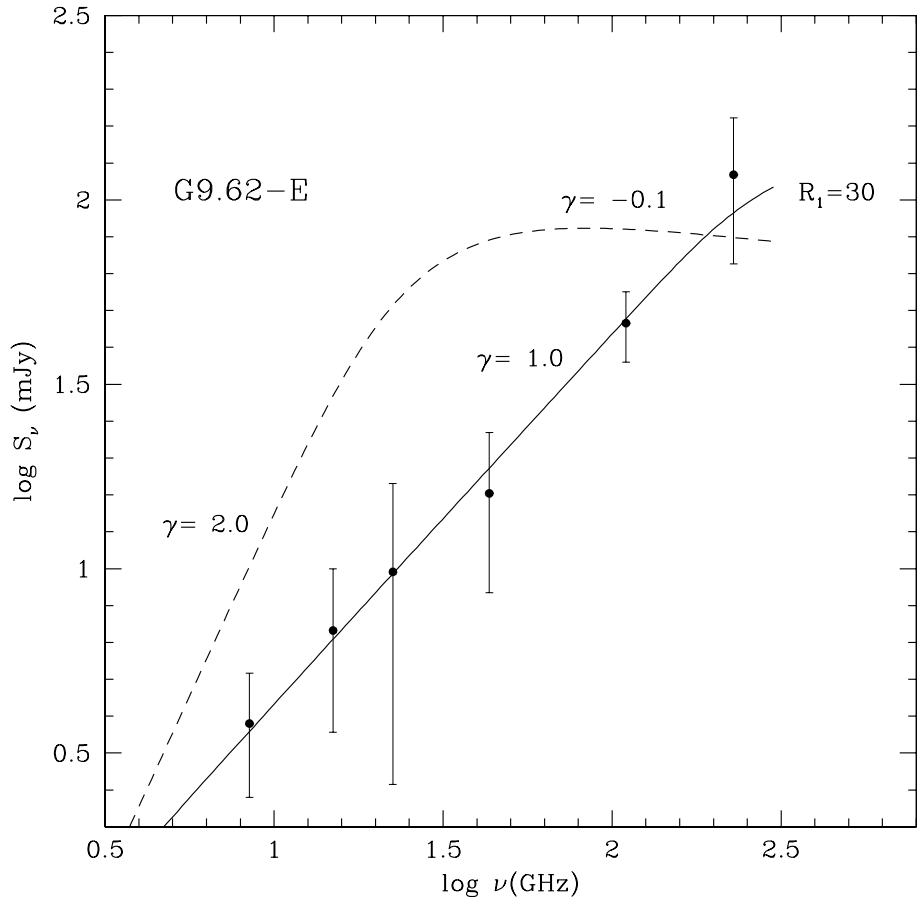

Figure 1: Spectrum of the HC HII G9.6-E. Model with density gradient ($n \propto r^{-2.6}$) and constant density.

Intermediate slope spectra have been explained as due to density gradients (Franco et al. 2000). Avalos et al. 2006 tested this hypothesis by looking at the predicted angular sizes as a function of frequency ($\theta \propto \nu^{-\delta}$, e.g., by Panagia & Felli 1975). This work was done for the HC HII regions G34.26+0.15 A and B, constraining the distribution of the ionized gas (shells).

High resolution 7mm images of some HC HII regions show limb brightening due to shells of ionized gas (Beltran et al. 2007; Sewilo et al. 2007; Avalos et al. [2007; see poster]). Simple models of these profiles indicate that the ionized gas is distributed in thick shells, with $\Delta \equiv (R_{\rm ext} - R_{\rm int})/R_{\rm ext} \sim 0.3 - 0.6$. These shells cannot be the result of the ionization of a shell swept-up a stellar wind because in that case, $\Delta \ll 1$.

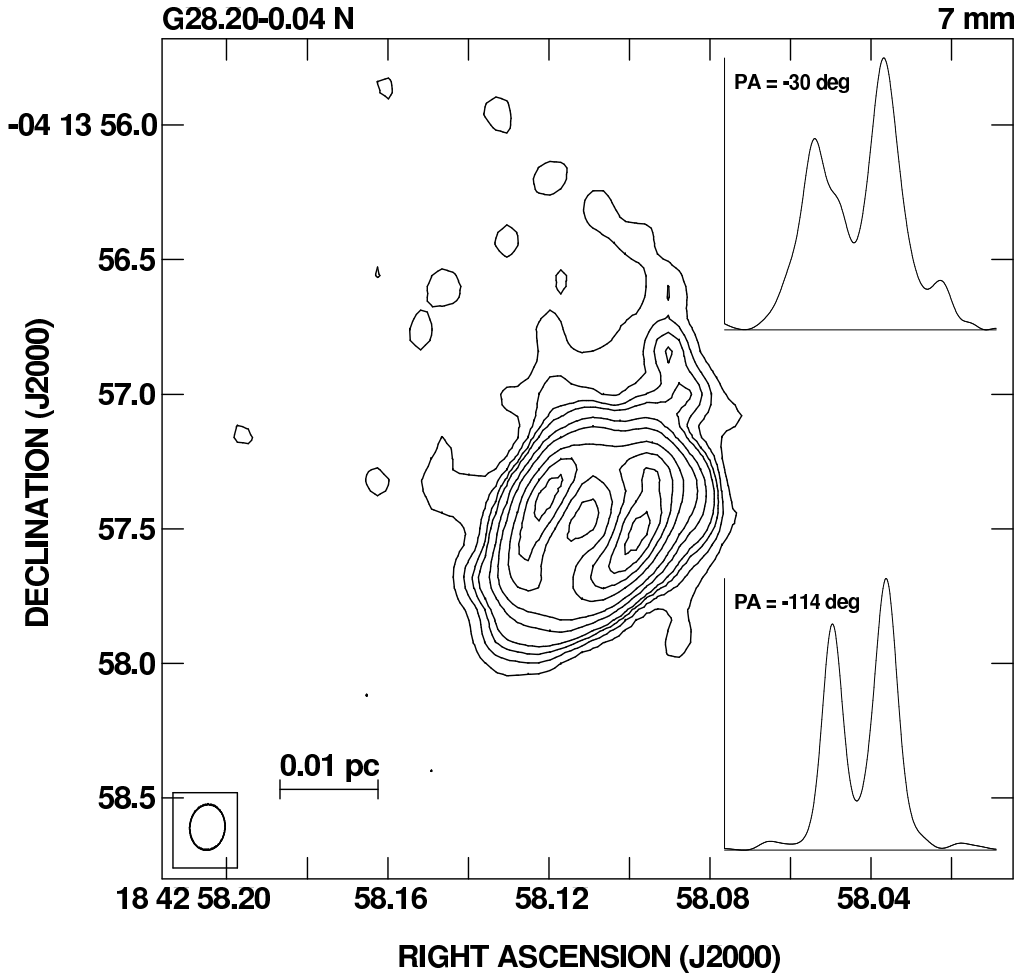

Figure 2: Expanding shell in G28.20+0.04N (Sewilo et al. (2007)).

Another model that can explain the observed intermediate slope spectra is a set of unresolved constant density clumps with a power law distribution of optical depths (Ignace & Churchwell 2004).

This model does not need to specify the spatial distribution of the clumps, thus, it does not address the issue of the observed intensity profiles and velocity fields.

Density gradients probably reflect the structure of flows because the crossing time of sound waves in HC HII regions is very small, $t \sim L/a = 1000$ yr.

- Expanding molecular shells have been found around W75N B and G24.78+0.08 A1 (Torrelles et al. (2003); Moscadelli et al. (2007)).
- Sewilo et al. (2007) find a velocity gradient in the line centroids of the H53α RRL across G28.20-0.04N.
- Keto et al. (2007) find evidence in several HC HII regions of redshifted/blueshifted gas comparing line centroids of RRLs at different frequencies (Welch & Marr (1987)).
- Gaume et al (1995) found the the RRL H66α in NGC7538 IRS 1 has $\Delta v > 150$ km/s. Lugo et al. (2005) modeled the spectrum of this source as a photoevaporated disk wind.

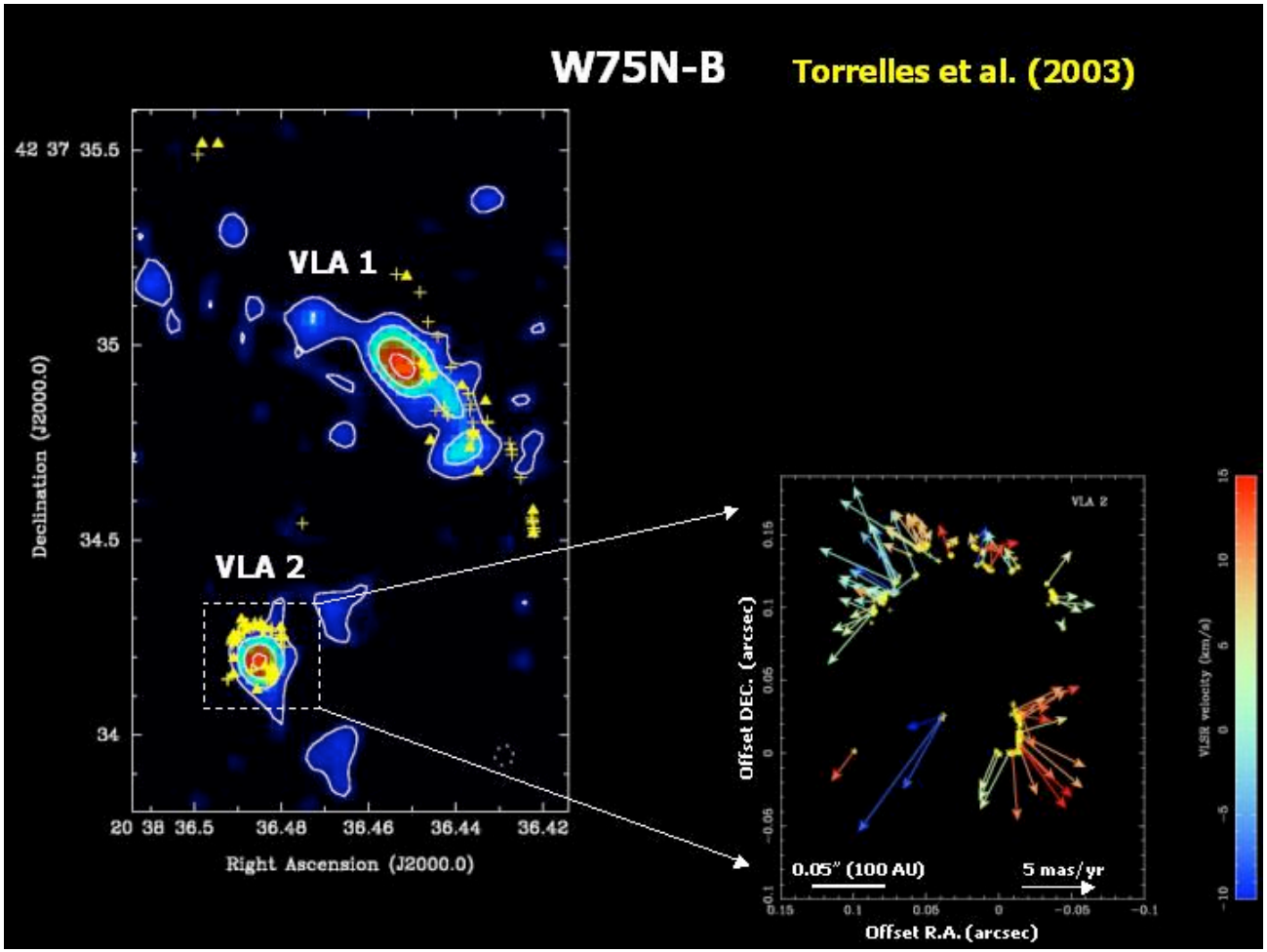

Figure 3: Expanding molecular shell of W75N B: proper motions of H_20 and methanol masers (Torrelles et al. (2003)).

Dust in HC HII regions

Dust in radiative equilibrium around a B0 star has a temperature $T \epsilon [200, 400]$ K in radii $r \epsilon [500, 1500]$ AU. The dust opacity at 1 mm is $\tau_d = 0.1 \left(\frac{\lambda}{200\mu m}\right)^{-1} \rho\ L = 1 \times 10^{-3} \ll 1$, for $n = 10^6 \mathrm{cm}^{-3}$ and $L \sim 5000$ AU.

In the Rayleigh limit, assuming a slab with $T = 300$ K,

$$S_\nu = B_\nu(T_d)\tau_\nu\Omega = 6\ mJy\ \left(\frac{\theta}{1"}\right)^2.$$

Assuming spherical symmetry and taking into account the temperature gradient, the dust emission 1 mm is even smaller (Sánchez et al. 2007). Nevertheless, even in high spatial resolution observations, mm emission toward HC HII regions will include dust along the l.o.s.

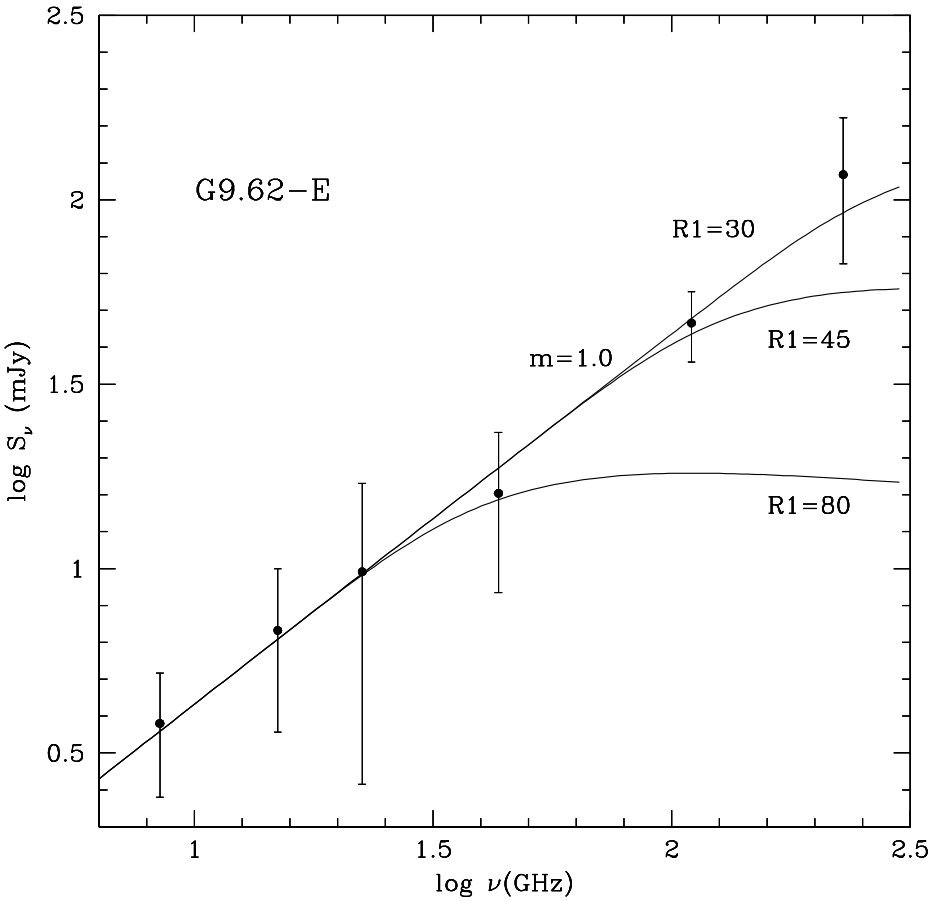

Figure 4: Spectrum of the HC HII G9.6-E and models with different inner radii.

Moreover, given the high densities of HC HII regions, if the dust-to-gas ratio is the same as that of the ISM $\Rightarrow$

$$\tau_d = \sigma_d n R_s = 41 \left(\frac{n}{10^6\,\mathrm{cm}^{-3}}\right)^{1/3} \left(\frac{S_*}{10^{49}\,\mathrm{s}^{-1}}\right)^{1/3}.$$

Thus, ionizing photons are immediately absorbed and the ionized region is truncated, i.e., there can be no "normal" dust inside HC HII regions ($R \sim 2000 - 3000$ AU).

This is in agreement with Keto & Kurtz (2007) who observed RRLs at high frequency with SMA (230 GHz) which requieres a high level of the free-free continuum.

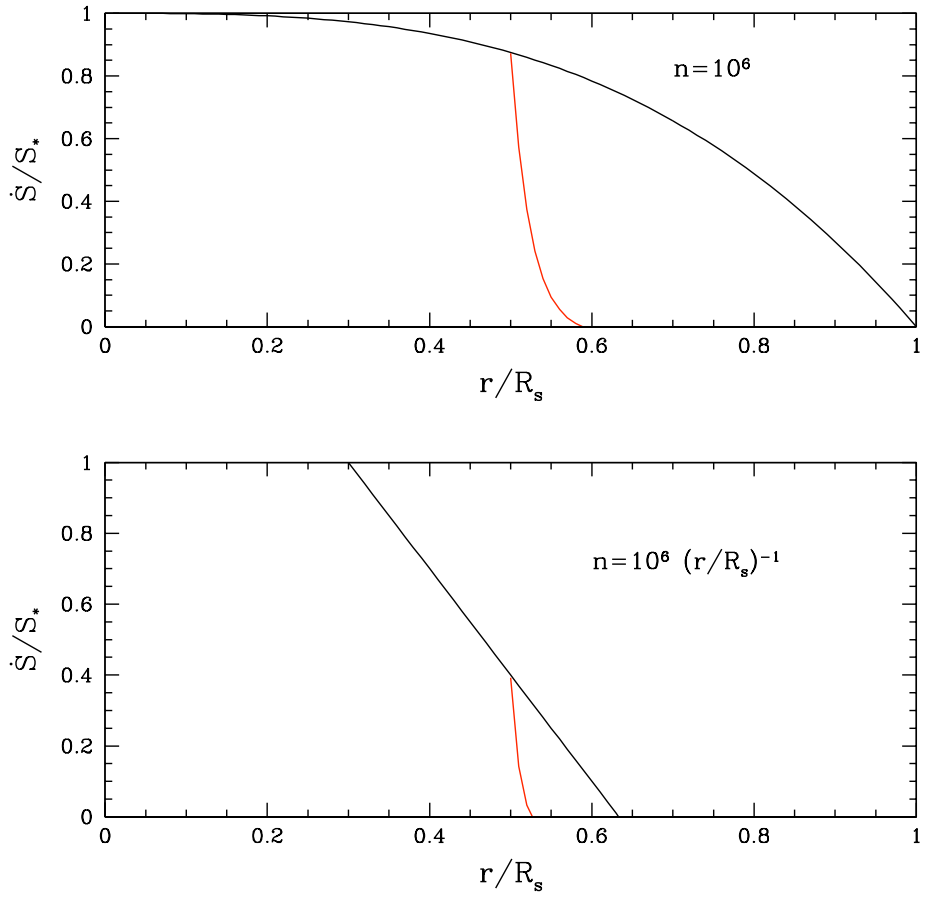

Figure 5: Effect of dust in the rate of ionizing photons. The models have $R_s = 1400$ AU, $\tau_d = 41$ (Sánchez et al. (2007)).

Why is there no dust inside HC HII regions?

- Radiation pressure on dust grains: for the high densities of HC HII regions, $P_{rad} > P_{gas}$. Since $a = \frac{L_\star \kappa}{4\pi r^2 c}$, where $\kappa \sim \sigma_d/\mu$, one can estimate

$$\frac{t_{pr}}{t_{cross}} \sim 0.03 \left(\frac{R_2}{1500\mathrm{AU}}\right)^{-1/2} \left(\frac{R_1}{100\mathrm{AU}}\right),$$

  i.e., the dust will be efficiently expelled from the HC HII region.

- Gas - dust coupling: the dust will couple to the gas via collisions. Nevertheless, $T_d \sim T_{sub} \Rightarrow n > 10^9\,\mathrm{cm}^{-3}$.

Models

If HC HII regions have ionized flows, there are some models that can apply to these regions:

- Ionized accretion flows
- Photoevaporated disks
- Mass loaded winds
- Champagne flows

Ionized Accretion Flow

A massive star forming in an accretion flow with $n \propto r^{-3/2}$ will ionized this flow up to the radius of ionization equilibrium, r_i. If

$$r_i < r_g \equiv \frac{GM_*}{a^2} = 180\,\mathrm{AU}\left(\frac{M_*}{20M_\odot}\right),$$

the HII region can be trapped in the accretion flow (Keto (2002); Keto & Wood (2006)).

Nevertheless,

$$r_g \sim 0.''1\left(\frac{M_*}{20M_\odot}\right)\left(\frac{D}{2\mathrm{kpc}}\right)^{-1},$$

smaller than the observed radii of resolved HC HII regions, unless the gravitational mass is larger.

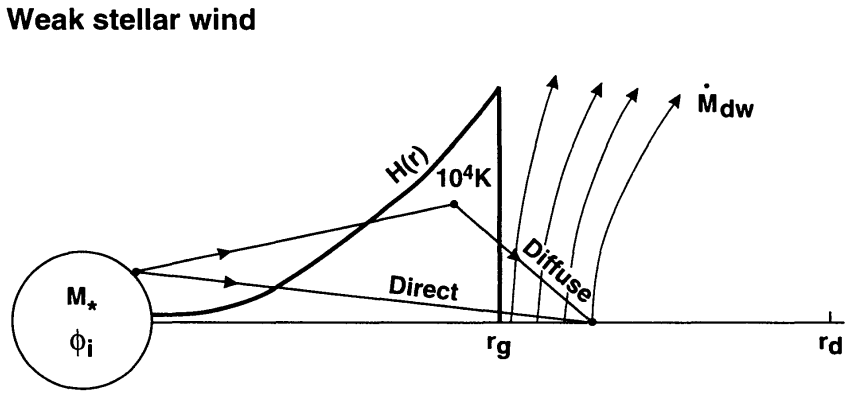

FIG. 1*a*

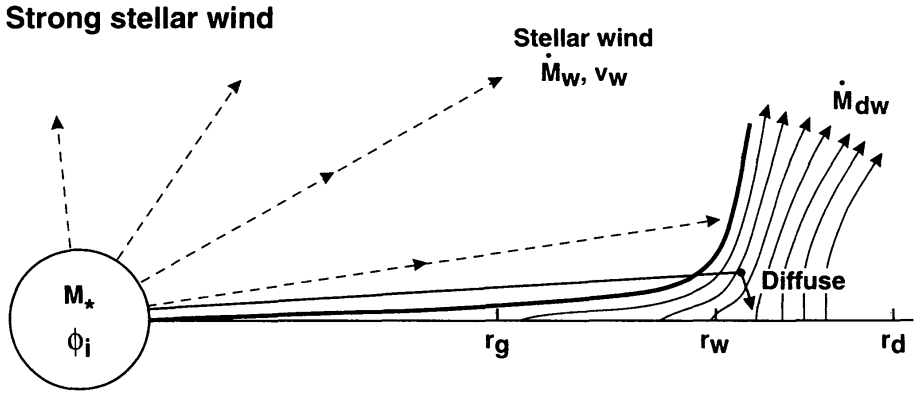

FIG. 1*b*

Figure 6: Photoevaporated winds from disks, e.g., NGC7538 IRS 1 (Hollenbach et al. 1994; Lugo et al. (2004)).

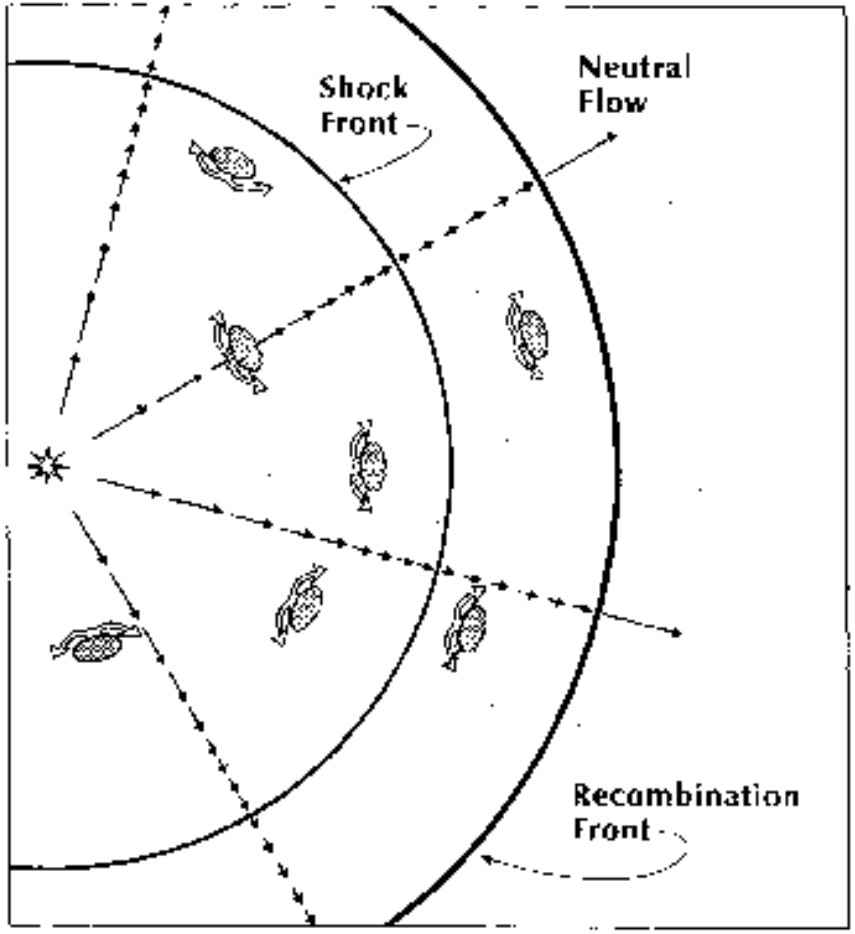

Mass loaded winds (Lizano et al. 1996). Scaled to the conditions of HC HII regions, the mass loaded subsonic region has

- $R_2 \sim 1500$ AU;
- $(R_2 - R_1)/R_2 \sim 0.4$;
- $n \sim 6 \times 10^5 \mathrm{cm}^{-3}$.

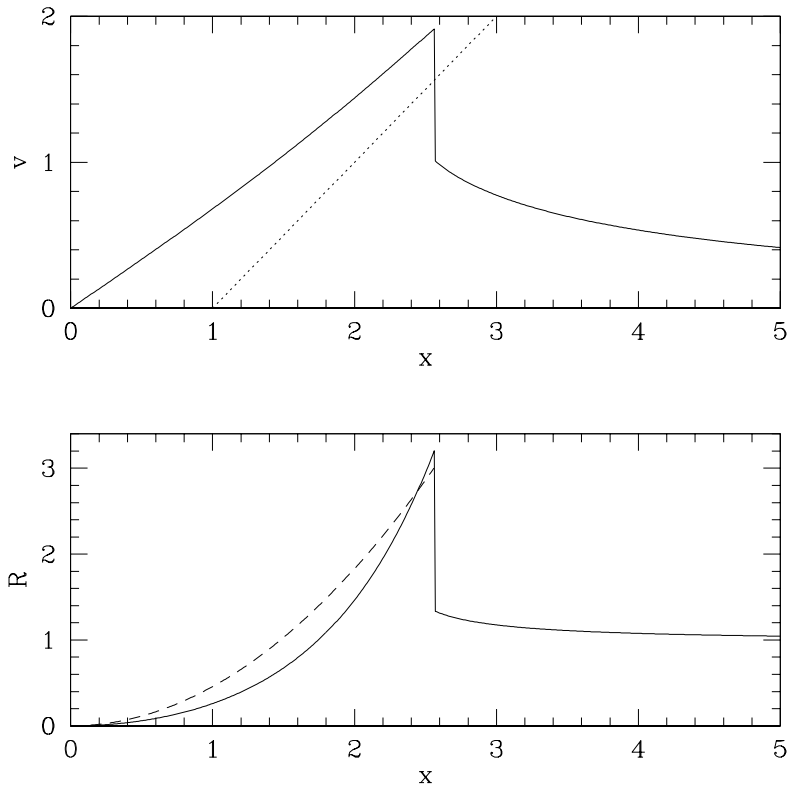

Figure 7: Champagne flow for $n \propto r^{-2}$. The solution is self-similar and the velocity of the shock is $v_s = a x_{\rm sh} \sim 26$ km/s (Shu et al. 2002).

Conclusions

- Information about the dynamics of HC HII will determine the origin and evolution of this phase in the life of massive stars.
- High resolution and high frequency RRL studies and methanol/H_20 maser studies are starting to give velocity information about these sources.
- Molecular lines in absorption against the free-free continuum with high spatial resolution are important diagnostics.
- RRL predictions of the models are needed.

.

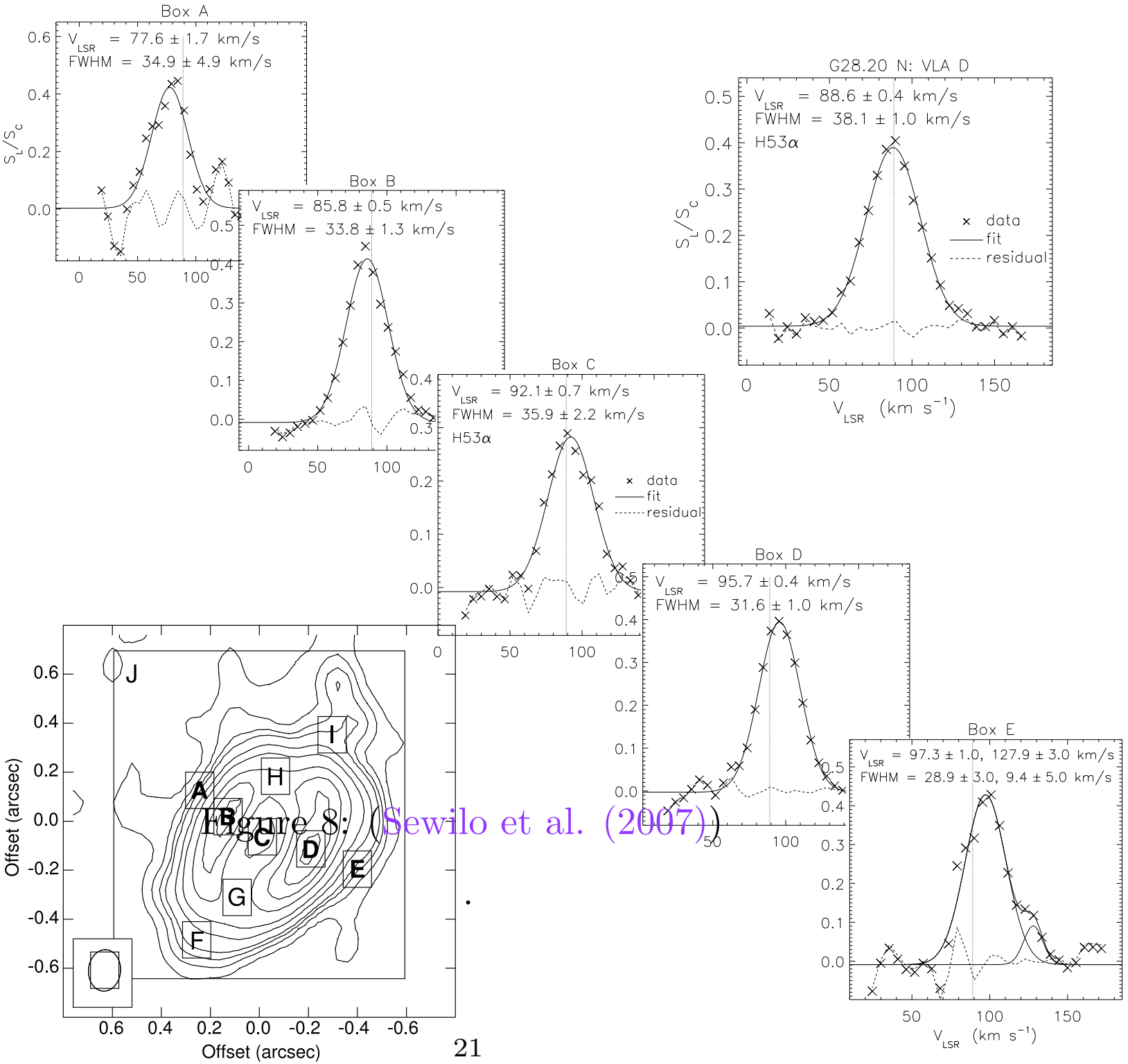

Figure 8: (Sewilo et al. (2007))

.

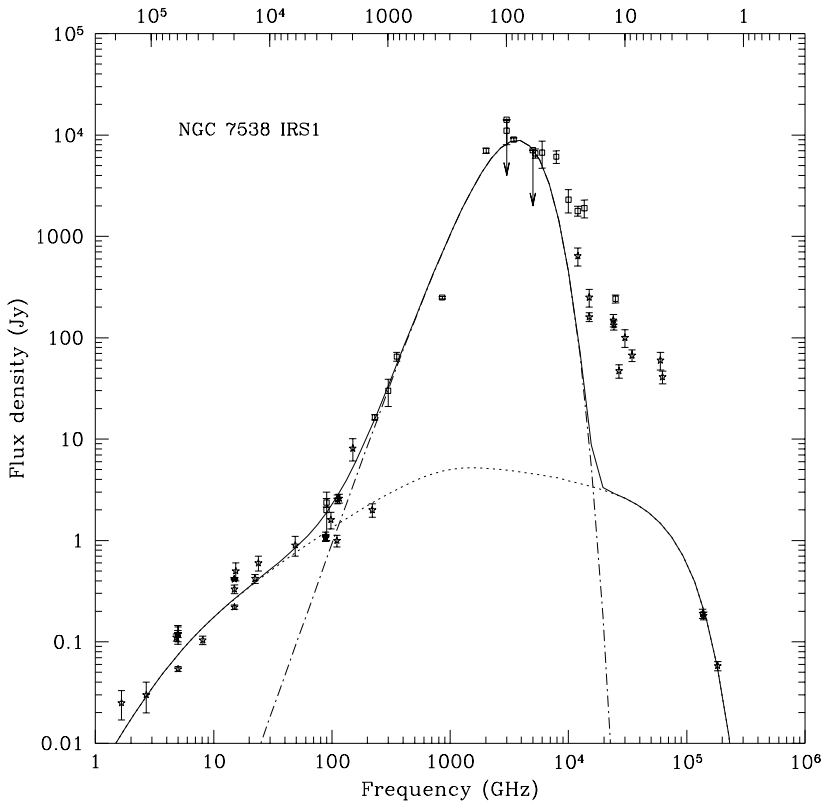

Figure 9: NGC7538 IRS1 has a bipolar morphology, wide RRLs, and was modeled as a photoevaporated wind (Lugo et al. (2004))

.

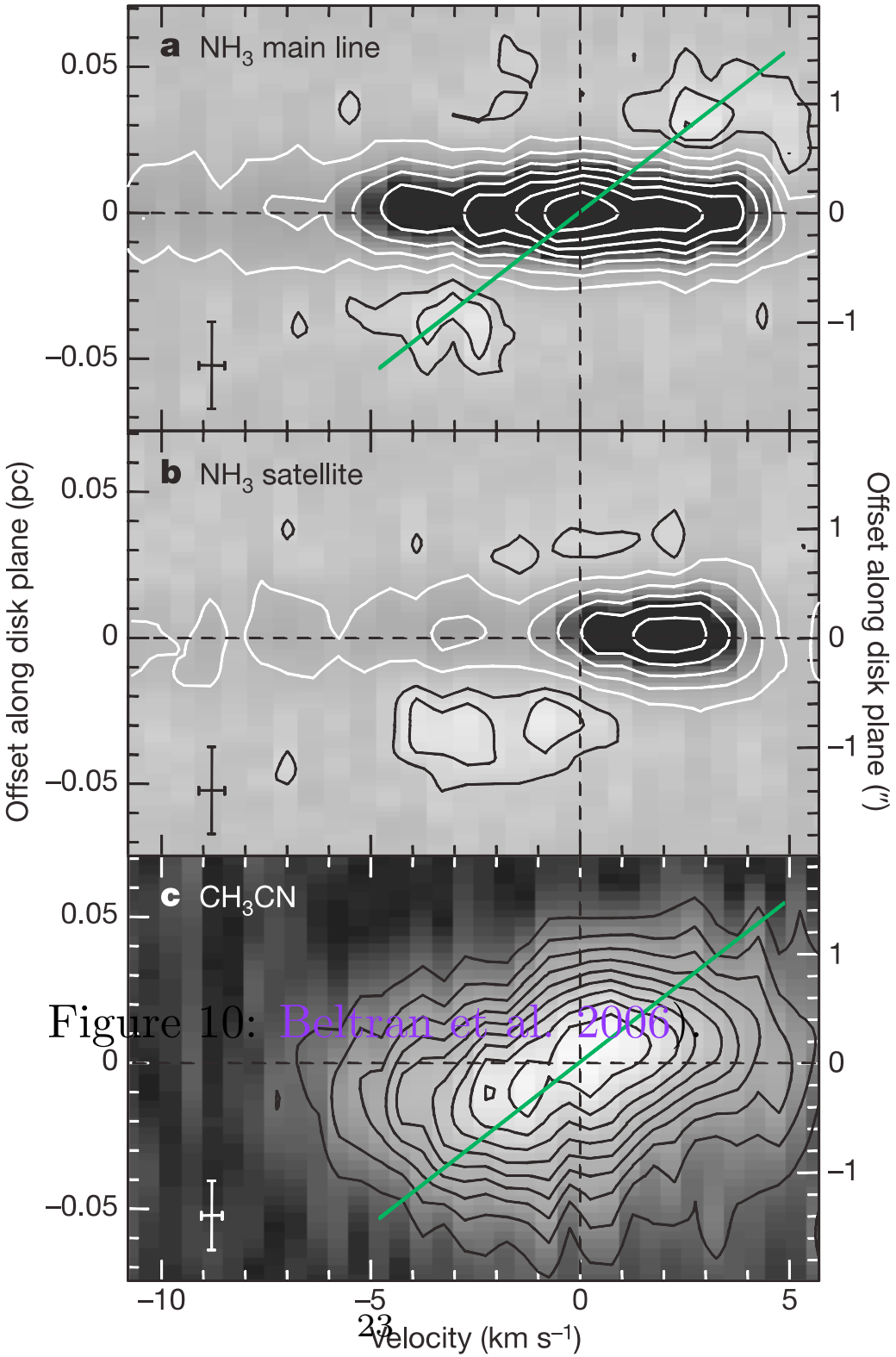

Figure 10: Beltran et al. 2006).

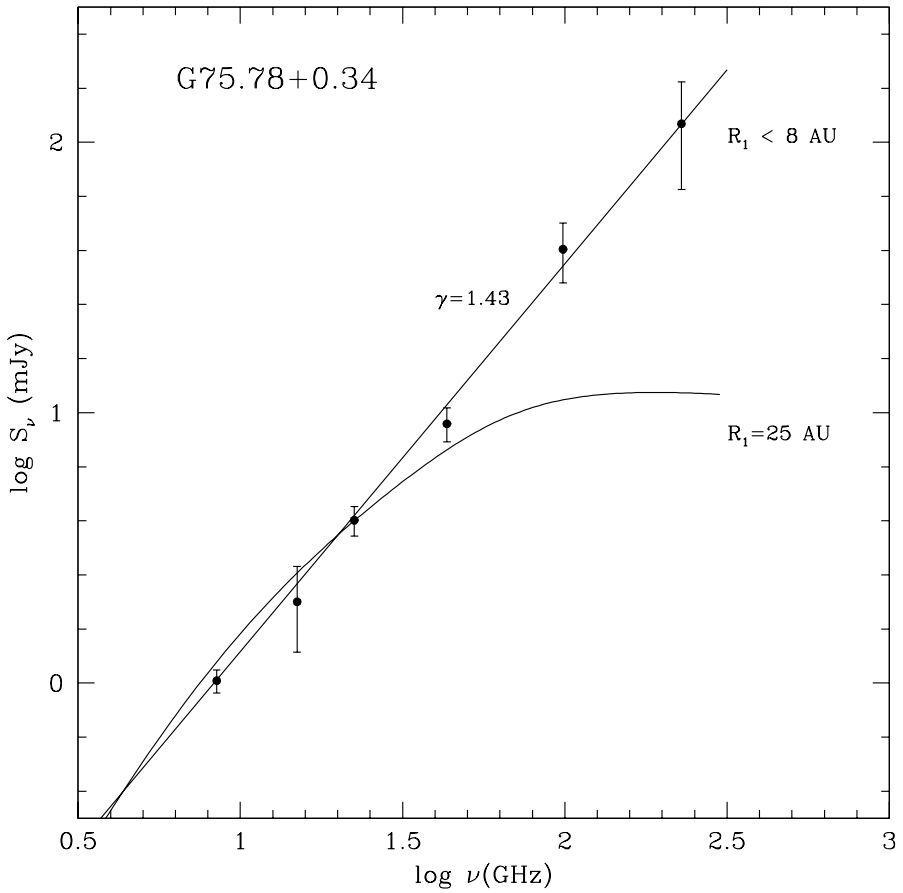

Figure 11: Spectrum of G75.78+0.34. Solid lines, shell models with inner radius $R_1 < 8 - 25$ AU, and outer radius, $R_2 \sim 150$ AU.